



Research Article

Performance evaluation of a rotary dryer in both co-current and counter-current configurations

Asmae ECHEERI^{1*}, Mostafa MAALMI^{1,2}

¹School of Engineers, Mohammed V University in Rabat, Rabat, Morocco

²Department of Process Engineering, Higher National School of Mines of Rabat, Rabat, Morocco

ARTICLE INFO

Article history

Received: 15 September 2020

Accepted: 10 February 2021

Keywords:

Co-current, Counter-current, Energy and exergy analysis, Mathematical model, Rotary dryer, Superphosphate fertilizer

ABSTRACT

A mathematical model was developed to simulate the process of superphosphates fertilizers drying in a rotary dryer in both co-current and counter-current configurations. Besides, the performance of the rotary dryer, installed in a local industrial unit, was assessed using the concept of energy and exergy analysis. Matlab software was used to develop the mathematical model, which is based mainly on mass and energy conservation equations. Good agreement between the simulated results and the experimental results from literature was obtained. The simulation results showed that the product's moisture content was reduced from an initial value of 0,14 kgH₂O / kg dry solid to 0.0912 and 0.0862 kgH₂O / kg dry solid at the dryer's outlet for the co-current and the counter-current configurations, respectively. A parametric study was carried out to evaluate the effect of the length of the dryer and the inlet drying air temperature on the moisture content to compare both configurations. Energetic and exergetic indicators were formulated and then computed based on the inlet operating conditions. The energy efficiency and the specific energy consumption for the co-current and the counter-current configurations were, respectively, found to be 13% and 24% and 5762 and 3502 kJ per kg of water evaporated. The exergy indicators, namely the exergy loss, the exergy destruction rate, and the exergetic efficiency, were 11.37 and 17.82 kW, 1.026 and 1.098 kW, 25.86 and 41.38% for the co-current and the counter-current configuration, respectively. A sensitivity analysis was used to investigate the effect of varying the inlet drying air temperature on energetic and exergetic performance parameters.

Cite this article as: Asmae E, Mostafa M. Performance evaluation of a rotary dryer in both co-current and counter-current configurations. J Ther Eng 2021;7(Supp 14):1945–1957.

INTRODUCTION

Drying is a process where moisture is reduced by evaporation to achieve a certain limit. In developed countries, drying operations consume about 12% of the industrial

energy [1]. For these reasons, drying has been a challenge for engineers and researchers, and the optimization of this process has to be of primordial importance. Despite the

***Corresponding author.**

*E-mail address: asmae.echeeri@gmail.com

This paper was recommended for publication in revised form by Regional Editor Mohammad Ghalambaz



availability of newer and more specialized dryers, rotary dryers are often considered as a typical example of modern engineering applications [2]. They are still used in the process industry, especially when the solid is in granular form and is not friable [3]. They can handle a variety of solids, such as fertilizers, sugar, cement, and others. The rotary dryer consists of a large, inclined cylindrical drum rotating around its axis slightly inclined on the horizontal; the heating can either be carried out directly and indirectly [4]. Rotary dryers include three transport phenomena: solids transportation, heat transfer, and mass transfer [5]. The most important aspect of drying technology is the mathematical modeling of the process. It requires using constitutive equations, such as the drying kinetics and the heat and mass exchange equations between the solid and gas phases. Many researchers have studied the problem of modeling the drying processes in different ways. A lot of them have tackled many detailed theoretical studies from different angles. Many highlighted the difficulties in obtaining a general drying model. They indicated their need to use empirical correlations specific to the materials to be dried and specific installations. Other scholars gave more interest to the experimental methods for studying the drying characteristics due to mathematical models' complexity. Douglas et al. [6] presented a dynamic sugar drying model in a counter-current flow rotary dryer. Cao and Langrish [7] modeled a counter-current rotary dryer based on the mass and energy balances combined with two subsidiary models. Iguaz et al. [8] proposed a dynamic model to simulate vegetable waste's drying process in a rotary dryer. Zabaniotou [9] investigated the influence of some input parameters on residence time and final moisture content of biomass. Xu and Pang [10] developed a mathematical model to simulate the drying of woody biomass in a rotary dryer running at a co-current and a counter-current flow to compare the two modes of operation. Castaño et al. [11] carried out a co-current rotary dryer based on basic general equations and correlations, allowing systematized modeling to study certain parameters' impact on the air temperature and the water content of the product at the outlet of the dryer. Hamed Abbasfard et al. [12] also developed a mathematical model of a co-current rotary dryer used to dry ammonium nitrate. In another paper [13], they studied the drying of ammonium nitrate using a co-current rotary dryer following a counter-current rotary dryer to optimize the factors that influence the performance of dryers. Carlos A. Bustamante et al. [14] proposed an overall design algorithm for a rotary dryer based on well-known correlations and energy and mass balances. They verified the overall dimensions first obtained from experimental data. Arruda [15] compared the performance of a conventional cascading rotary dryer with a modified configuration, known as a roto-aerated dryer used for drying particle fertilizers. In another study [16], they analyzed heat and mass transfer modeling between the air and the particles of

superphosphate fertilizers in co-current and counter-current configurations and compared with experimental data results. Silva et al. [5] believed that it is important to analyze the sensitivity of the model's responses proposed by Arruda et al. [16] to the variation of the input parameters. Souza et al. [17] analyzed heat and mass transfer between soybean seeds and the air in the so-called roto aerated dryer in recent work. Qu et al. [2] explored an experimental method for evaluating a corncob's drying characteristics in a plate rotary heat exchanger. They studied the influence of several parameters on the maximum drying rate. Simona et al. [18] evaluated the drying process of biomass in a rotary dryer. They investigated the effect of inlet parameters on the moisture content of the dried material the temperature profiles along the dryer's length.

Although the rotary dryer structure appears simple, the drying process is very complicated and requires the optimization of energy sources to improve the drying performance and energy efficiency. Furthermore, the design of an energy-intensive system, as the drying process, for higher efficiency and lower cost is the main goal for sustainable development. Energy analysis is considered a basic tool to evaluate energy conversion processes [19]. Due to its inability to give more details about thermodynamic processes' irreversibility aspects, attention is given to exergy analysis of drying processes and systems. The exergy analysis's main objective is to quantify the sources of inefficiencies, distinguish the quality of energy consumption, and select optimal drying conditions [20]. In this context, Mortaza et al. [20] gave an overview of the application of exergy analysis in drying processes and facilities in various drying systems. Yogesh Kumar and Vinkel Arora [21] reviewed the tools for energy and exergy analysis applied to drying systems and explained the procedure to implement and factors affecting them. In recent years, many sectors showed an interest in energy and exergy analysis. D. Peinado et al. [22] studied the energy and exergy analysis of a rotary dryer employed in a hot mix asphalt plant to heat and dry the aggregates. W. Rong et al. [23] evaluated the thermodynamic performance of a rotary kiln-electric furnace using the exergy analysis method to quantify the process's irreversibilities. Yali Wong et al. [24] assessed a roller kiln's thermal performance based on energy and exergy analysis using the operating values from a ceramic factory. A. Ustaoglu [25] carried out energy and exergy analyses of a rotary kiln and cooling section in a cement plant using a wet process. An organic Rankine Cycle is proposed to recover the capacity of exhausted gases. In the same context, J.A. Adeniran et al. [26] conducted an exergy analysis and air pollutants emission estimation of a rotary kiln system in a cement manufacturing plant. They presented a possible heat recovery system and CO₂ mitigation approaches. Neslihan Colak [27] studied the performance of a four-step industrial pasta drying system using the exergy analysis method and evaluated the effect of some variables on drying performance. Topic [28] presented a

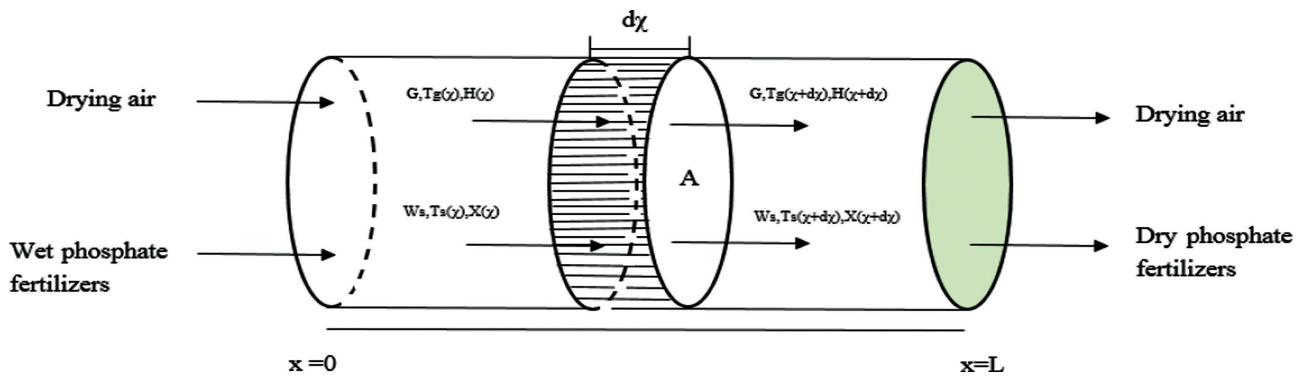


Figure 1. Schematic illustration of a rotary dryer operating at a co-current flow.

mathematical model for exergy analysis of an industrial high-temperature forage dryer. Other authors [29] [30] presented the energy and exergy analysis of drying systems used to dry vegetable slices and evaluated the impact of some experimental variables on the exergy efficiency and the overall exergy loss system. Hassan Sheikhshoaei [31] identified the main sources of exergy destruction for the pistachio roasting plant. A new method is recently applied, combining artificial neural network methods with exergy analysis in drying systems [32-33]. However, this method is more complicated than the conventional exergy analysis used previously.

To the best of our knowledge, few articles assessed the comparison between two configurations of the rotary dryer (co-current and counter-current) based on mathematical modeling. Besides, little is known about evaluating the performance of rotary dryers based on the energy and exergy analysis. Furthermore, it was noticed that the work on energy and exergy analysis with fertilizers is not reported; products on which the emphasis was placed in previous studies are cement, wood chips, vegetable slices, pasta, etc... For this purpose, the objective of this work is to assess the mathematical modeling of a rotary dryer of superphosphate fertilizers and evaluate the influence of some input parameters on the drying of the product. The study is carried out for both co-current and counter-current configurations, and a comparison between them is made. For model validation, numerical simulation results are compared with the experimental results from the literature [15]. This work [15] presents an ideal candidate for comparison due to the similarity of the studied systems. On the other hand, energy and exergy analysis of the drying system under study in both configurations is carried out to gain better insight to the drying process and evaluate its thermodynamic performance. A parametric study is conducted by varying the inlet drying air temperature to determine if it affects the energetic and exergetic indicators, namely the energy efficiency, the specific energy consumption, the exergy destruction rate and the exergetic efficiency.

MATERIALS AND METHODS

Materials

Superphosphate is a phosphate mineral fertilizer. It is one of the world's most important fertilizer sand and is involved in various plants' metabolic processes. Indeed, it is important for their roots and their growth. The particles used in this study are fertilizers in the form of simple superphosphate granules [15], and the drying gas used is air. The inlet operating conditions of fertilizers and gas are listed in table 1.

The industrial rotary dryer considered in the present work is presented in figure 1. It is a sheet metal cylinder slowly rotating about a slightly inclined axis. A number of flights are placed along the cylinder to ensure a better transfer of heat and mass between the drying material and the air. The characteristics of the rotary dryer are listed in table 1.

Mathematical Modeling

The drying process modeling in a rotary dryer is based on the application of the conservation equations of mass and energy on the two phases present in the dryer, namely: the fluid and the particles to be dried. These equations are applied, in a stationary state, on an infinitesimal element of the dryer. In formulating this model, the following assumptions are made:

- The particles of the product have a spherical geometry, and their dimensions remain unchanged;
- The drying process takes place only in the falling rate period;
- The physicochemical properties of the solid phase do not change during drying;
- The initial conditions of superphosphate fertilizers, moisture and the temperature of the particles and air are known;
- For each dryer volume element, the product input flowrate is equal to the product output flowrate of the previous volume element;

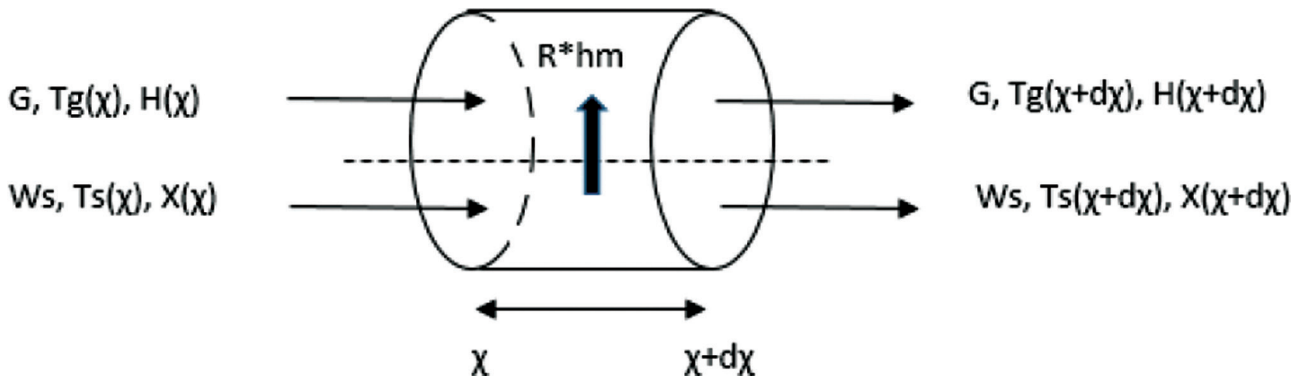


Figure 2. Schematic diagram of the infinitesimal volume element of the rotary dryer operating at co-current flow.

- The axial particle velocity through the drum is constant;
- The plug flow is assumed for the fluid;
- The reference temperature and pressure do not change with time;
- The principle of the ideal gas mixture is used for gases in the system;
- The kinetic and potential energy and exergy of materials are negligible.

CONSTITUTIVE EQUATIONS

heat and mass balances

The differential equations system obtained from the conservation of mass and energy between drying gas (air) and particles (superphosphates fertilizers) is presented below, where χ is the reduced variable (dimensionless length), given by the proportion between a given position z and the total length of the dryer L . Fig.2 shows the schematic diagram of an infinitesimal volume element of the rotary dryer (shown in Fig. 1) operating at co-current flow.

Mass balances in both solid and air in the volume element at dimensionless abscise χ :

$$\frac{dX}{d\chi} = -\frac{R * h_m}{Ws} \quad (1)$$

$$\frac{dH}{d\chi} = \frac{R * h_m}{G} \quad (2)$$

Energy balances on both solid and air in the volume element at dimensionless abscise χ :

$$\frac{dT_s}{d\chi} = \frac{Uva * V * (Tg - Ts) - \lambda * R * h_m}{Ws * (c_{ps} + X * c_{pa})} \quad (3)$$

$$\frac{dTg}{d\chi} = \frac{-Uva * V * (Tg - Ts) - c_{pv} * R * h_m * (Tg - Ts)}{G * (c_{pg} + H * c_{pv})} - \frac{Up * A * (Tg - Tamb)}{G * (c_{pg} + H * c_{pv})} \quad (4)$$

The system of these four differential equations represents the mathematical model of the study. It can be solved numerically, knowing the drying rate equation and the residence time, to determine the profiles of the following parameters: the water content of the product, the humidity of the air, and the outlet temperature of both the air and the solid product. In the above equations, h_m is the total mass load (hold-up). It is defined as the product of the solid flow rate Ws and the average residence time τ . For the counter-current configurations, the mass and energy balance equations are the same with adjustment of the sign of the first term of each equation.

drying kinetics and equilibrium moisture

Arruda et al. [15] conducted a statistical study based on experimental data of the simple superphosphate fertilizers' equilibrium moisture content in a thin layer dryer. They concluded that the best correlation to describe the equilibrium moisture is:

$$X_e = \left(\frac{-\exp(-0,045 * Ts - 0,28)}{\ln(RH)} \right)^{\frac{1}{1,435}} \quad (5)$$

Where RH is the relative humidity determined from the air saturation data:

$$RH = \frac{H}{0,0028 * \exp(0,0701 * Tg)} \quad (6)$$

For the drying kinetics, Arruda et al. [10] concluded that the best correlation is:

$$R = \frac{(1 - XR) * (X_i - X_e)}{\tau} \quad (7)$$

Where XR is dimensionless solid moisture, called moisture ratio, it is given by:

$$XR = \frac{X - X_e}{X_i - X_e} = \exp\left(-0,431 * \exp\left(\frac{-121,845}{Tg}\right) * \tau^{0,392}\right) \quad (8)$$

heat transfer coefficients

The best correlation allowing the calculation of volumetric heat transfer coefficient Uva in a rotary dryer has been proposed by Arruda [34]. It is expressed as follows:

$$Uva = 0,394 * \left(\frac{G}{A}\right)^{0,289} * \left(\frac{Ws}{A}\right)^{0,541} \quad (9)$$

For the heat loss coefficient, it is expressed by:

$$Up = \left(\frac{1}{h_e} + \frac{e}{K_{th}} + \frac{1}{h_i}\right)^{-1} \quad (10)$$

residence time

The residence time is one of the most important design parameters that define the rotary dryer performance. However, there is no general model that best describes solids' residence time in rotary dryers. In this study, the empirical correlation used for calculating residence time is the one proposed by Friedman and Marshall [35]. It is written as follows:

$$\tau = 0,3 * \left(\frac{0,23 * L}{tg(s) * n^{0,9} * d} - \frac{0,6 * 5 * (d_p^{0,5}) * L * G}{Ws}\right) \quad (11)$$

other thermal properties

The majority of works carried out in mathematical modeling of rotary dryers consider that the drying air and water's physicochemical properties and the latent heat of vaporization don't change during drying. In this paper, and for more calculations accuracy, the specific heat of air and water and latent heat of vaporization aren't constant and are calculated by correlations from literature data [36] [37]:

$$c_{pg} = \frac{0,78 * (3,115 * 10^{-1} - 1,357 * 10^{-2} * Tf + 2,68 * 10^{-5} * Tf^2 - 1,168 * 10^{-8} * Tf^3 + 0,22 * (2,714 * 10 + 9,274 * 10^{-3} * Tf - 1,381 * 10^{-5} * Tf^2 + 7,645 * 10^{-9} * Tf^3)}{29} \quad (12)$$

$$c_{pa} = \frac{3,224 * 10 + 1,924 * 10^{-3} * Ts + 1,055 * 10^{-5} * Ts^2 - 3,596 * 10^{-9} * Ts^3}{18} \quad (13)$$

Latent heat of vaporization is calculated by the following expression obtained from tabulated data:

$$\lambda = -0,0074 * Ts^2 - 0,00925 * Ts + 2424,7 \quad (14)$$

drying moisture efficiency

Most previous works evaluate the efficiency of drying or compare the performances of different configurations by determining the final moisture content of the product. This gives an idea about how efficient is the drying process but has to refer often to the initial moisture content of the product.

In this work, a new indicator is defined as drying moisture efficiency. It is a dimensionless number, defined as the ratio between the amounts of free water evaporated from a given solid during the drying operation on the product's initial moisture content. It gives information about the efficiency of drying regardless of the initial moisture content. It is expressed as:

$$\eta_{drying} = \frac{X_i - X_f}{X_i} * 100 \quad (15)$$

NUMERICAL SIMULATION

For the co-current configuration, the method of integration used for ordinary differential equations is the series of methods called Runge-Kutta fourth and five orders. It is modeled on the Matlab software as the integrated function "ode45". An initial value problem was solved using a Matlab code since all boundary conditions are at the same point. The boundary conditions are:

$$X(\chi=0) = X_i; \quad H(\chi=0) = H_i \\ Ts(\chi=0) = Ts_i; \quad Tg(\chi=0) = Tg_i$$

The equations of the counter-current configuration present boundary value problems (BVP). The integration method is the finite difference method, which starts the solution with an initial guess supplied at an initial mesh point and changes step-size to get the specified accuracy. This was done with the help of the Matlab solver "bvp4c". In this case, the given order of BVP is defined on the interval [0, 1] subject to two-point boundary conditions as:

$$X(\chi=0) = X_i; \quad H(\chi=1) = H_i \\ Ts(\chi=0) = Ts_i; \quad Tg(\chi=1) = Tg_i$$

Table 1. Initial operating conditions and Industrial rotary dryer characteristics, in a local industrial unit in Safi Morocco, used in the simulation of the rotary dryer for co-current and counter-current flow

	Properties	Unit	Value
Ws	Dry solid mass flow rate	kg/s	0.125
G	Air mass flow rate	kg/s	0.55
H _i	Initial Air absolutehumidity	kgwater/kg dry air	0.01
X _i	Initial Solid moisture	kgH2O/kg dry solid	0.14
T _{s_i}	Initial solid temperature	°C	125
T _{g_i}	Initial gas temperature	°C	300
T _{amb}	Ambiant temperature	°C	25
L	Dryer length	m	8
D	Dryer diameter	m	1
d _p	Particle diameter	m	2.45*10 ⁻³
S	Dryer slope	degrees	26
N	Dryer rotation speed	rad/s	2.61*10 ⁻²
A	Dryer cross-sectional area	m ²	0.785
V	Dryer volume	m ³	6.28
c _{ps}	Specific heat of dry solid	kJ/kg.°C	1.02508
c _{pv}	Specific heat of water vapor	kJ/kg.°C	1

For model simulation, initial operating conditions and dryer configuration data are presented in Table1.

ENERGY AND EXERGY ANALYSES

Generally, the analysis of transformation processes involves collecting measures, the definition of performance indicators, the calculation of these indicators, and the evaluation of performances based on the indicator's results. This analysis is then used as a basis for identifying process improvements and efficiency potentials. To this end, the energy and exergy analyses of the drying process use a number of indicators to evaluate the process's energy and exergy performances. In this section, the efficiency of superphosphates fertilizers drying in a rotary dryer is evaluated based on energy and exergy analysis. Generally, the most common way to evaluate energy efficiency is by determining the amounts of energy used and the energy consumed per amount of water evaporated. Indeed, these parameters don't necessarily give a detailed overview of energy efficiency in drying. For this purpose, exergy analysis is fundamental for the drying process. Thus, other indicators are considered, namely the exergy efficiency and the exergy destruction rate. This evaluation method will be applied to two different configurations of the rotary dryer, namely co-current and counter-current configurations, and a comparison between them will be made.

Energy Analysis

The energy analysis is based on the first law of thermodynamics. In steady-state conditions, the energy balance can be expressed as :

$$\sum En_i = \sum En_e \quad (16)$$

$$\sum m_e * h_e - \sum m_i * h_i = Q - W \quad (17)$$

Where m is the mass flow rate; Q refers to the heat transfer rate; W represents the power; h indicates the specific enthalpy. The subscripts i and e denote the control volume inlet and outlet, respectively.

For the rotary dryer, the energy balance can be written as :

$$En_{air,i} + En_{wp} = En_{air,e} + En_{dp} + Q_{loss} \quad (18)$$

The energy efficiency can be defined as the ratio between the total energy consumed to the maximum theoretical energy that can be expected from it [37]. It is expressed as:

$$\eta_{energy} = \frac{Q}{G * (c_{pgi} + H_i * c_{pv}) * (Tg_i - Tamb)} * 100 \quad (19)$$

Another indicator can be calculated called specific energy consumption E_{sc}. It measures the amount of

energy used to evaporate one kilogram of water. It can be expressed as:

$$E_{sc} = \frac{Q}{Ws * (X_i - X_f)} \quad (20)$$

This indicator is more significant than the energy efficiency as it permits to determine the dryer’s thermal efficiency contrary to the energy efficiency; the latter gives only an idea about the energy used during the drying but not necessarily how efficient is the drying process.

Exergetic Analysis

The exergy theory defines an integrated analysis method that encompasses the first two principles of thermodynamics and thus makes it possible to take into account both the quantity and the quality of energy involved. The concept of exergy is defined as the maximum amount of work produced by a system or a flow of matter or energy as it comes to equilibrium with a reference environment [38]. The exergy differs from energy in that the latter is preserved while exergy is destroyed whenever irreversibilities exist. The exergy analysis identifies the thermodynamic irreversibilities and allows the quantitative evaluation of thermal imperfections.

The general exergy balance is expressed as:

$$\sum Ex_i = \sum Ex_e + \sum Ex_d \quad (21)$$

Where Ex_i and Ex_e are the exergy rate of input and output flows, respectively, and Ex_d is the exergy rate destruction.

For the rotary dryer, the exergy balance is written as:

$$Ex_{air,i} + Ex_{wp} = Ex_{air,e} + Ex_{wp} + Ex_{loss} + Ex_d \quad (22)$$

The total exergy of a system is defined as:

$$Ex = Ex_{physical} + Ex_{kinetics} + Ex_{chemical} + Ex_{potential} \quad (23)$$

Generally and for many engineering applications (including rotary dryers and similar processes), kinetic, potential, and chemical exergy are negligible. Thus:

$$Ex = Ex_{physical} = m * [H - H_0 - T_0 * (S - S_0)] \quad (24)$$

Where m, H, and S denote, respectively, the mass flow rate, the enthalpy and entropy of the system at the specified state, and H_0 and S_0 are the values of the same properties when the system is at the restricted dead state.

The exergy rate associated with the drying air at different points in the rotary dryer is [39]:

$$Ex_a = G * cp_{gi} * Tamb * \left\{ \frac{Tg_i}{Tamb} - 1 - \ln\left(\frac{Tg_i}{Tamb}\right) + \frac{K-1}{K} * \left[\ln\left(\frac{P}{Pamb}\right) + \frac{Tg_i}{Tamb} * \left(\frac{Pamb}{P}\right) - 1 \right] \right\} \quad (25)$$

Where K is the specific heat ratio

The exergy rate of the product can be expressed as [30] [41]:

$$Ex_p = Ws * cp_s * \left[T_s - T_0 - T_0 * \ln\left(\frac{T_s}{T_0}\right) \right] \quad (26)$$

The exergy efficiency is the ratio between the exergy gained to total exergy paid. The exergy gained is defined as the exergy of evaporation. The exergy paid is the exergy input. It is defined by [39]:

$$\eta_{exergetic} = \frac{Ex_i - Ex_e}{Ex_i} * 100 \quad (27)$$

RESULTS AND DISCUSSION

The simulation results are illustrated in Fig.2, 3, 4, and 5 show product moisture content, product temperature, and air temperature profiles along the dryer.

Figures 3 and 4 show the results obtained for the co-current rotary dryer. From Figure 3, the product moisture content decreases linearly along with the dryer and reaches a final moisture content around 0.0912 kgH2O / kg dry solid after drying from an initial value of 0,14 kgH2O / kg dry solid. The temperatures of the two streams in the co-current

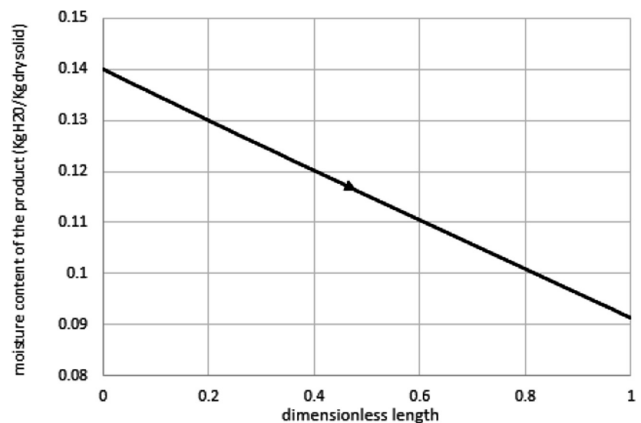


Figure 3. Solid moisture profile for the rotary drying operating at co-current flow.

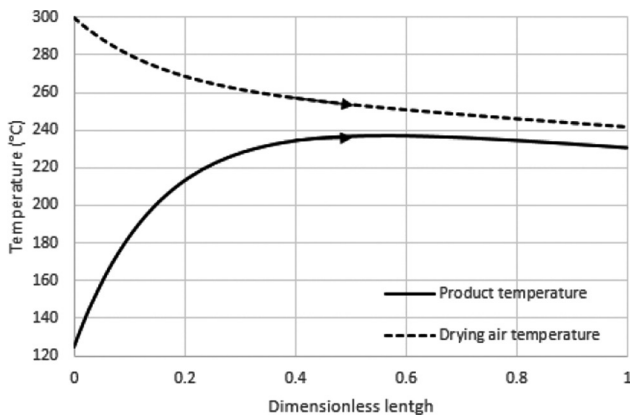


Figure 4. Product and drying air temperature profiles for the rotary drying operating at co-current flow.

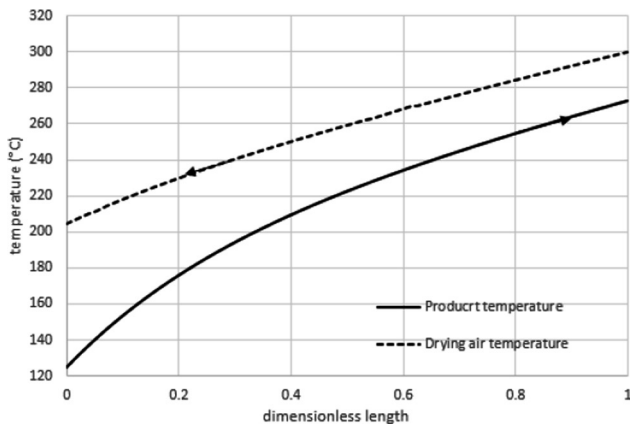


Figure 6. Product and drying air temperature profiles for the rotary drying operating at counter-current flow.

rotary dryer are shown in Fig.4. They are different at the inlet of the dryer but get closer along with the dryer; it reaches 242°C for the air and 231°C for the fertilizers; this is typical behavior co-current system with heat exchange. Fig. 5 and 6 show the simulation results for drying in the counter-current rotary dryer.

From Fig.5, the product moisture content decreases linearly along with the dryer and reaches a final moisture content around 0.0862 kgH₂O / kg drysolid. Fig.6 illustrates the temperature profiles of the two streams along the dryer length. The temperature of the product increases exponentially and reaches 273°C at the outlet of the dryer. As for the air temperature, it reaches 204°C at the outlet of the dryer with a heat driving force relatively constant in the whole dryer. From these results, it can be seen that for the same operating conditions, the counter-current rotary dryer dries the product to final moisture lower than the final moisture

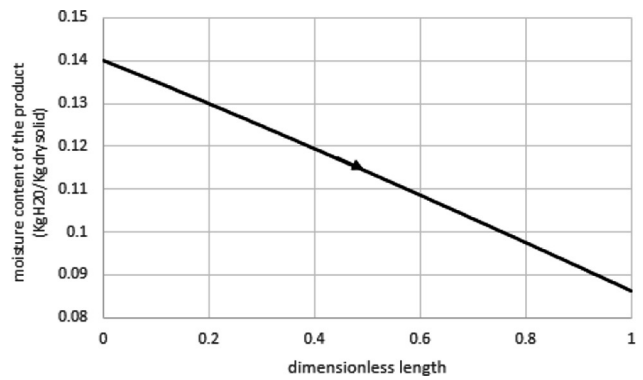


Figure 5. Solid moisture profile for the rotary drying operating at counter-current flow.

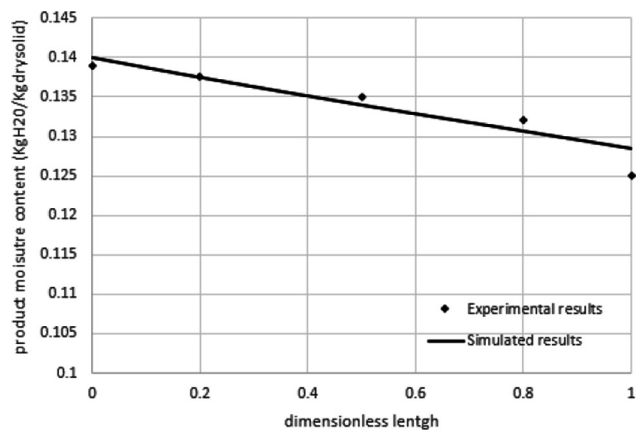


Figure 7. Experimental and simulated results of the product moisture content profiles for the rotary drying operating at counter-current flow [15].

obtained at the outlet of the co-current configuration. This indicates that more energy is transferred from the hot air to the product in the counter-current dryer with a lower outlet air temperature. For the case studied here, the product's final moisture content at the outlet of the dryer operating at co-current flow (8m) is reached in the counter-current configuration for a length of 7.28 m. Thus, the required dryer length for the counter-current configuration is shorter than the co-current configuration for the product's same target moisture content. To achieve the same target moisture content obtained at the counter-current configuration (0.0862 kg H₂O / kg dry solid) in the rotary dryer operating at co-current flow, one of the following parameters must be increased:

- The size of the dryer from 8 to 11.2 m (40 % increase);
- The temperature of the drying air from 300 to 410° C (36.7% increase).

Thus, the variations established on the system's parameters at co-current flow require a higher energy expenditure, which shows that the counter-current configuration is the most efficient.

Figures 7 and 8 show the comparison between results computed by the model (counter-current configuration) and experimental profiles [15] to ensure the model's validity. A good agreement is observed between the two profiles of product moisture content and product temperature. The average deviation of the simulation results with the experimental data was 0.86 % for the product moisture content and 3.08% for the product temperature, which are very good results if we consider that small errors always accompany experimental data.

The following figures present the results of drying moisture efficiency, energy and exergy analysis for several operating conditions by varying the drying air's inlet temperature.

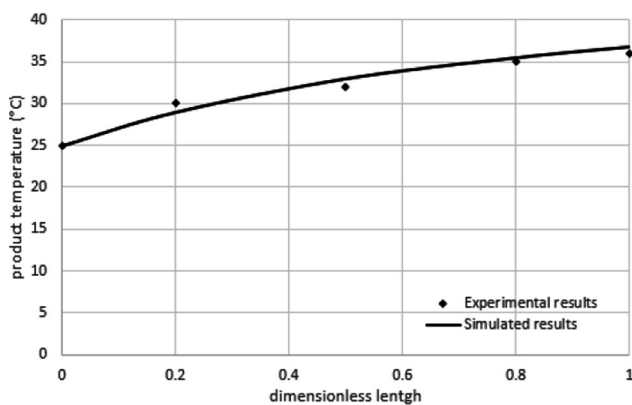


Figure 8. Experimental and simulated results of the product temperature profiles for the rotary drying operating at counter-current flow [15].

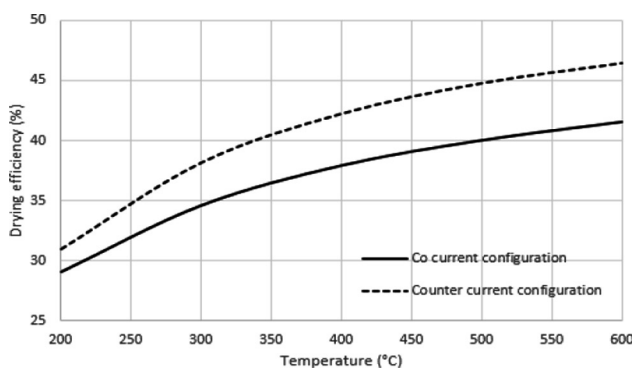


Figure 9. Simulated results of the variation of drying moisture efficiency.

The variation of drying moisture efficiency is shown in Fig.9. It increases with inlet drying air temperature for both co-current and counter-current configuration. For the case studied ($T_g = 300^\circ\text{C}$), the co-current configuration's drying efficiency is 34.6% and for the counter-current configuration it is 38%. So, the counter-current configuration allows better drying of the product for the same amount of energy consumed. As it can be seen in Fig.10, energy efficiency increases exponentially with drying air temperature. At $T = 300^\circ\text{C}$, its values for the co-current and counter-current flows are 13% and 24%, respectively. Thus, the highest value of energy efficiency occurs in the counter-current configuration. It means that more energy is used according to the definition of energy efficiency. Another indicator is used to evaluate the rotary dryer's energy performances and is more significant, called the specific energy consumption and given by equation (20). As shown in Fig.11, the evolution of specific energy consumption for both configurations is very similar.

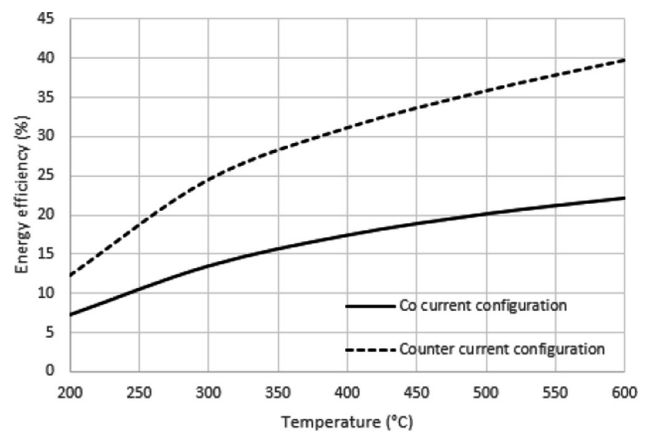


Figure 10. Simulated results of the variation of energy efficiency.

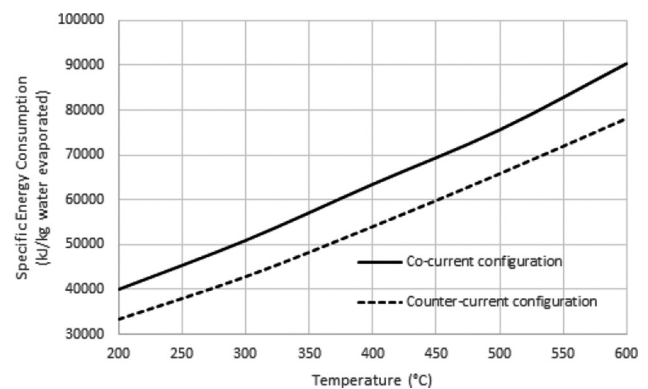


Figure 11. Simulated results of the variation of specific energy consumption.

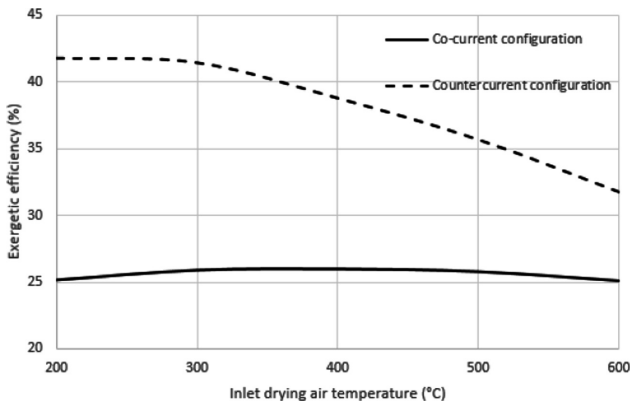


Figure 12. Simulated results of the variation of exergy efficiency.

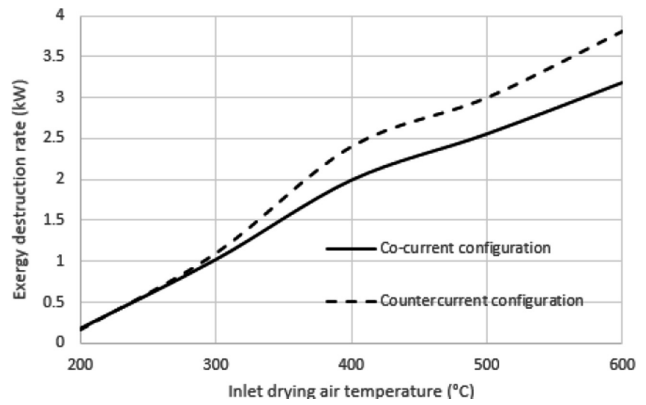


Figure 13. Simulated results of the variation of the exergy destruction rate.

The counter-current configuration has lower values of the specific energy consumption than the co-current while increasing temperature. Thus, it can be concluded that the counter-current configuration uses less energy for the same amount of water evaporated. Although the difference in energy efficiency becomes important at a higher temperature, the difference in specific energy consumption remains the same. So the drying moisture efficiency and the specific energy consumption are better correlated than the energy efficiency criterion.

Exergy parameters of the rotary dryer in both configurations are grouped in table 2. They are calculated based on the inlet operating conditions figured in table 1.

It is seen that the exergy loss of the rotary dryer in the co-current and the counter-current configurations are 11.37 kW and 17.83 kW, respectively. It's noteworthy that the overall exergy loss rate amounts to 24% and 39% of the total exergy input for the co-current and the counter-current configurations, respectively. The higher value of the exergy loss rate in the counter-current configuration compared with the co-current can be attributed to the high heat transfer in the counter-current configuration. These losses can be reduced through thermal insulation.

The rotary dryer presents little irreversibilities. Indeed the overall exergy destruction rate for the co-current and the counter-current configuration is 1.026 kW and 1.099 KW. It represents 2.14% and 2.4% respectively of the exergy input to the rotary dryer. This means that a small amount of exergy input to the dryer is dissipated because of heat and mass transfer phenomena.

Exergy efficiency values are 25.86% and 41.39% for the co-current and the counter-current configuration, respectively. A small portion of the exergy input for the co-current rotary dryer is utilized for moisture removal from the fertilizers compared to the counter-current configuration. It is justified because most of the exergy input is lost due to

Table 2. Exergetic parameters of the rotary dryer

	Co-current configuration	Counter-current configuration
Exergy input rate (kW)	47.93	45.73
Exergy output rate (kW)	35.53	26.80
Exergy loss (kW)	11.37	17.83
Exergy destruction rate (Kw)	1.026	1.099
Exergy efficiency (%)	25.86	41.39

irreversibilities and thermal losses in the co-current configuration. Besides, exergy efficiency in the counter-current is higher than in the co-current because of the high exergy destruction rate during mass and heat transfer from the drying air to the product.

Figure 11 illustrates the variation of the evolution of exergy efficiency with increasing inlet drying air temperature. As it can be seen, the profile of the exergetic efficiency remains almost constant at 25,5% while varying the drying air temperature in the co-current configuration and decreases from 41,73% to 31,72% in the counter-current configuration. Indeed, other researchers [37] [42] [43] reported that exergy efficiency decreases with increasing drying air temperature. For the co-current configuration, the exergy efficiency doesn't vary substantially with temperature because the energy efficiency also varies slightly with temperature compared to the counter-current case. The exergy destruction rate values increased as the inlet drying air temperature increased (figure 13). Thus, it can be concluded that the use of lower drying air temperature contributes to increase the exergy usage and to reduce thermodynamic irreversibilities allowing more efficient use of available energy in the drying air.

Nevertheless, the increase of the drying air temperature to accelerate heat transfer and the evaporation of water is not thermodynamically justified because of the higher exergy destruction rate and, therefore, decreased exergy efficiency. This is why the energy efficiency in Fig.9 increases faster for the counter-current than the co-current without contributing to bigger drying efficiency. The counter-current dryer presents good results in terms of drying performance, energy, and exergy efficiency. Nevertheless, it should be noted that the co-current configuration is also frequently used when the product to be dried is temperature-sensitive and must not be heated to high temperature at the dryer outlet.

CONCLUSION

In this study, a mathematical model of a rotary dryer in both co-current and counter-current configurations is developed to simulate the drying of superphosphate fertilizers and to evaluate the influence of some parameters on the drying of the product. The model developed can be used to simulate any rotary dryer in both configurations for drying a granular solid, the necessary specific inputs are the solid drying kinetics and the equilibrium moisture data. Comparison between results computed by the model simulation for the counter-current configuration and experimental profiles [10] shows very good agreement. Furthermore, energetic and exergetic analyses of the dryer under study were performed to give a better insight into its thermodynamic performance. A sensitivity analysis was used to investigate the effect of varying the inlet drying air temperature on energetic and exergetic indicators. The main conclusions drawn from the results of the present study are:

- the moisture content of the product reaches lower value after drying in the counter-current configuration than in the co-current one;
- The required dryer length for the counter-current configuration is shorter by 40% than the co-current configuration for the same target moisture content of the product;
- The inlet drying air temperature, must be increased in the co-current configuration by 36.7% to achieve the same target moisture content obtained at the counter-current configuration;
- The drying moisture efficiency is higher for the counter-current configuration with a value 38% compared to 34.6% for the co-current configuration.
- While increasing the inlet drying air temperature, the counter-current configuration has lower values of the specific energy consumption than the co-current one. Thus, for the same amount of water evaporated, the counter-current configuration uses less energy.
- The overall exergy destruction rate for the co-current and the counter-current represents 2.14% and 2.4% respectively of the exergy input to the rotary dryer.

For the exergy efficiency, values are 25.86% and 41.39% for the co-current and the counter-current configuration, respectively. A small portion of the exergy input to the co-current rotary dryer is utilized for moisture removal from the fertilizers compared to the counter-current configuration. This result is justified because most of the exergy input is lost due to irreversibilities and thermal losses in the co-current configuration;

- Drying moisture efficiency, energy efficiency, and specific heat consumption and exergy destruction rate increase while increasing the inlet drying air temperature in both configurations. Thus, the use of lower drying air temperature contributes to increase the exergy usage and to reduce thermodynamic irreversibilities;
- The exergy efficiency remains almost constant while varying the inlet drying air temperature in the co-current configuration and decreases in the counter-current one; so the exergy analysis gives a better insight on how the energy is used during the drying process.

NOMENCLATURE

C_{pa}	Specific heat of pure water	$\text{kJ/kg}\cdot^{\circ}\text{C}$
C_{pg}	Specific heat of dry air	$\text{kJ/kg}\cdot^{\circ}\text{C}$
E_{sc}	Specific energy consumption	$\text{kJ/kgwater evaporated}$
E	Thickness	m
En	Energy	kW
Ex	Exergy	kW
h_m	Dryer total load	kg
P	Pressure	atm
Q	Total energy consumed	kJ
R	Dryer rate	$\text{Kg water/kg dry solid/s}$
R_g	Constant of the ideal gas	$\text{J/mol}\cdot\text{K}$
RH	Air relative humidity	-
t	Time	s
Up	Heat loss coefficient	$\text{kW/m}^2\cdot^{\circ}\text{C}$
Uva	Global volumetric heat transfer coefficient	$\text{kW/m}^2\cdot^{\circ}\text{C}$
XR	Dimensionless moisture	-
x	Mole fraction	-

Greek symbols

χ	Dimensionless length
Λ	Latent heat of vaporization
τ	Average residence time
η	Efficiency

Subscripts

Amb	Ambient
F	Final

<i>V</i>	Water vapor
<i>G</i>	Gas
<i>I</i>	Initial
<i>S</i>	Solid
<i>wp</i>	Wet product
<i>dp</i>	Dry product
<i>d</i>	Destruction

AUTHORSHIP CONTRIBUTIONS

Authors equally contributed to this work.

DATA AVAILABILITY STATEMENT

The authors confirm that the data that supports the findings of this study are available within the article. Raw data that support the finding of this study are available from the corresponding author, upon reasonable request.

CONFLICT OF INTEREST

The author declared no potential conflicts of interest with respect to the research, authorship, and/or publication of this article.

ETHICS

There are no ethical issues with the publication of this manuscript.

REFERENCES

- [1] Mujumdar AS, Handbook of Industrial Drying. 3rd ed. New York: Marcel Dekker; 2006.
- [2] Qi C, Huang Y, Ling X, Duan L. Experimental study on drying characteristics of corncob in plant rotary heat exchanger. *J Food Process Eng* 2019;42:e13059. [\[CrossRef\]](#)
- [3] Silverio BC, Soares ACC, Arruda EB, Duarte CR, Barrozo MAS. Analysis of the influence of mini-pipes diameter in the performance of a non-conventional rotary dryer. *Mater Sci Forum* 2012;727-728:1890-1895. [\[CrossRef\]](#)
- [4] Ji Y, Li X, He J, Duan X. Drying efficiency and product quality of biomass drying: a review. *Dry Technol* 2020;38:2039-2054. [\[CrossRef\]](#)
- [5] Silva MG, Lira TS, Arruda EB, Murata VV. Modeling of fertilizer drying in a rotary dryer: parametric sensitivity analysis. *Brazil J Chem Eng* 2012;29:359-369. [\[CrossRef\]](#)
- [6] Douglas PL, Kwade A, Lee PL, Mallick SK. Simulation of a rotary dryer for sugar crystalline. *Dry Technol* 1993;11:129-155. [\[CrossRef\]](#)
- [7] Cao WF, Langrish TAG. The development and validation of a system model for a counter-current cascading rotary dryer. *Dry Technol* 2000;18:99-115. [\[CrossRef\]](#)
- [8] Iguaz A, Esnoz A, Martinez G, Lopez A, Virseda P. Mathematical modeling and simulation for the drying process of vegetable wholesale by-products in a rotary dryer. *J Food Eng* 2003;59:151-160. [\[CrossRef\]](#)
- [9] Zabaniotou AA. Simulation of forestry biomass drying in a rotary dryer. *Dry Technol* 2007;18:1415-1431.
- [10] Xu Q, Pang S. Mathematical modeling of rotary drying of woody biomass. *Dry Technol* 2008;26:1344-1350. [\[CrossRef\]](#)
- [11] Castaño F, Rubio FR, Orteha MG. Modeling of a cocurrent rotary dryer. *Dry Technol* 2012;30:839-849.
- [12] Abbasfard H, Ghader S, Rhafsanjani HH, Ghanbari M. Mathematical modeling and simulation of an industrial rotary dryer: A case study of ammonium nitrate plant. *Powder Technol* 2013;239:499-505. [\[CrossRef\]](#)
- [13] Abbasfard H, Ghader S, Rhafsanjani HH, Ghanbari M. Mathematical modeling and simulation of drying using two industrial cocurrent and counter-current rotary dryers for ammonium nitrate. *Dry Technol* 2013;31:1297-1306. [\[CrossRef\]](#)
- [14] Bustamante CA, Hill AF, Rodriguz DF, Giraldo M, Florez WH. Modeling and simulation of a cocurrent rotary dryer under steady conditions. *Dry Technol* 2014;32:469-475. [\[CrossRef\]](#)
- [15] Arruda EB, Lobato FS, Assis AJ, Barrozo MAS. Modeling of fertilizer drying in roto-aerated and conventional rotary dryers. *Dry Technol* 2009;27:1192-1198. [\[CrossRef\]](#)
- [16] Arruda EB, Façanha JMF, Pires LN, Assis, AJ, Barrozo MAS. Conventional and modified rotary dryer: Comparison of performance in fertilizer drying. *Chem Eng Process* 2009;48:1414-1418. [\[CrossRef\]](#)
- [17] Souza GFMV, Avendano PS, Francisquetti MCC, Ferreira FRC, Duarte CR, Barrozo MAS, Modeling of heat and mass transfer in a non-conventional rotary dryer. *Applied Thermal Engineering* 2021;182:116118.
- [18] Simona PL, Spuru P, Ion I, Mathematical modeling of the sawdust drying process for biomass pelleting. *Energy Procedia* 2017;141:150-154. [\[CrossRef\]](#)
- [19] Nazghelichi T, Aghbashlo M, Kianmehr MH. Optimization of an artificial neural network topology using coupled response surface methodology and genetic algorithm for fluidized bed drying. *Comput Electron Agric* 2011;75:84-91. [\[CrossRef\]](#)
- [20] Aghbashlo M, Mobli H, Rafiee S, Madadlou A. A review on exergy analysis of drying processes and systems. *Renew Sust Energy Rev* 2013;22:1-22. [\[CrossRef\]](#)
- [21] Kumar I, Arora VK, Energy and exergy analysis and its application of different drying techniques:

- a review. ISME Journal of Thermofluids 2019;5:10-29.
- [22] Peinado D, de Vega M, Garcia-Hernando N, Marugan-Cruiz C. Energy and exergy analysis in an asphalt plant's rotary dryer. Appl Therm Eng 2011;31:1039-1049. [\[CrossRef\]](#)
- [23] Rong W, Li B, Liu P, Qi F. Exergy assessment of a rotary kiln-electric furnace smelting of ferronickel alloy. Energy 2017;138:942-953. [\[CrossRef\]](#)
- [24] Wang Y, Yang H, Xu K. Thermal performance combined with cooling system parameters study for a roller kiln based on energy-exergy analysis. Energies 2020;13:3922. [\[CrossRef\]](#)
- [25] Ustaoglu A, Alptekin M, Emin Akay M. Thermal and exergetic approach to wet type rotary kiln process and evaluation of waste heat powered ORC (Organic Rankine Cycle). Appl Therm Eng 2017;112:281-295. [\[CrossRef\]](#)
- [26] Adeniran JA, Yusuf RO, Aremu AS, Aareola TM. Exergetic analysis and pollutants emission from a rotary kiln system in a major cement manufacturing plant. Energy and Environment 2018;30:601-616. [\[CrossRef\]](#)
- [27] Colak N, Erbay Z, Hepbasli A. Performance assessment and optimization of industrial pasta drying. Int J Energy Res 2013;37:913-922. [\[CrossRef\]](#)
- [28] Topic R. Mathematical model for exergy analysis of drying plants. Dry Technol 1995;13:437-545. [\[CrossRef\]](#)
- [29] Aghbashlo M, Kianmehr MH, Arabhosseini A. Performance analysis of drying of carrot slices in a semi-industrial continuous band dryer. J Food Eng 2009;91:99-108. [\[CrossRef\]](#)
- [30] Aghbashlo M, Kianmehr MH, Arabhosseini A. Energy and exergy analysis of thin-layer drying of potato slices in a semi-industrial continuous band dryer. Dry Technol 2008;26:1501-1508. [\[CrossRef\]](#)
- [31] Sheikhshoaei H, Dowlati M, Aghbashlo M, Rosen MA. Exergy analysis of a pistachio roasting system. Dry Technol 2019;38:1565-1583. [\[CrossRef\]](#)
- [32] Nikbakht AM, Motevali A, Minaei S. Energy and exergy investigation of microwave-assisted thin-layer drying of pomegranate arils using artificial neural networks and response surface methodology. J Saudi Soc Agric Sci 2014;13:81-91. [\[CrossRef\]](#)
- [33] Kaveh M, Abbaspour-Gilandeh Y, Chen G. Drying kinetic, quality, energy and exergy performance of hot air-rotary drum drying of green peas using adaptative nereu-fuzzy inference system. Food Bioprod Process 2020;124:168-183. [\[CrossRef\]](#)
- [34] Arruda EB. Comparison of the performance of the roto-fluidized dryer and conventional rotary dryer. Ph.D thesis. Federal University of Uberlandia, Uberlandia, Brasil, 2006.
- [35] Friedman S J, Marshall WRJ. Studies in rotary drying, part I: Holdup and dusting. Chemical Engineering Progress 1949a; 482-493.
- [36] Reid RC, Prausnitz JM, Poling BE. The Properties Of Gases & Liquids. 4th ed. New York: McGraw Hill: 1987: 656-668.
- [37] Syahrul S, Dincer I, Hamdullahpur F. Thermodynamic modeling of fluidized bed drying of moist particles. Int J Therm Sci 2003;42:691-701. [\[CrossRef\]](#)
- [38] Wang Z, Zhang Y, Zhang B, Yang F, Yu X, Zhao B, Wei Y. Analysis of energy consumption of the drying process for dried Chinese noodles. Appl Therm Eng 2017;110:941-948. [\[CrossRef\]](#)
- [39] Chowdhury MMI, Bala BK, Haque MA. Energy and exergy analysis of the solar drying of jackfruit leather. Biosyst Eng 2011;110:223-229. [\[CrossRef\]](#)
- [40] Bejan A, Tsatsaronis G, Moran MJ. Thermal Design and Optimization. Exergy Analysis. Hoboken: Wiley; 1995:113-116.
- [41] Ozgener L, Ozgener O. Exergy analysis of drying process, An experimental study in a solar greenhouse. Dry Technol 2009;27:580-586. [\[CrossRef\]](#)
- [42] Aghbashlo M, Mobli H, Rafiee S, Madadlou A. A review on exergy analysis of drying processes and systems. Renew Sust Energy Rev 2013;22:1-22. [\[CrossRef\]](#)
- [43] Sarker SH, Ibrahim MN, Aziz NA. Energy and exergy analysis of industrial fluidized bed drying of paddy. Energy 2015;84:131-138. [\[CrossRef\]](#)